Characterization and evaluation of thermal sprayed amorphous coating layers – Part I

S. Crâsteţi, D. R. Pascu, D. Buzdugan

National R&D Institute for Welding and Material Testing – ISIM Timişoara, Romania
E-mail: sandu@isim.ro

Keywords

Amorphous coating, thermal spraying, digital image processing

1. Introduction

In the modern industrialized societies an ever increasing need to reduce or control wear, general corrosion and fatigue, due to various reasons, like: an extension of the lifetime of the equipments, to produce more efficient motors and devices, to develop new advance products, to conserve the limited material resources, or to spare energy and increase safety.

In the recent years the research activities were aimed to control and reduce corrosion by using surface treatments and additional surface layers. Such objectives were also aimed in ISIM, in the frame of a project destined to obtain amorphous layers by thermal spraying, to ensure a dense coating layer free of pores and oxides, with a good adherence on the support material, finally allowing to obtain some new advanced materials having the desired working characteristics. These amorphous coating layers on support materials with poor characteristics do represent new materials with highly increased characteristics regarding tribologic, wear and corrosion resistance. This does lead to increased functional performances of certain products in the aeronautical and automotive industries.

The paper will further present the materials, procedures and results that were obtained so far in the research activities at ISIM Timisoara.

2. Choice of materials and the chemical compositions of the thermally sprayed coating layers

To benefit of a rapid cooling, aluminium was the choice for the base material, given its high thermal conductivity (λ = 237 W/mK). The chemical composition is shown in Table 1.

Table 1. Chemical composition of materials

Chemical composition (atomic percentage)					
Al		Fe		Cu	
Min.	Max.	Min.	Max.	Min.	Max.
99.59	99.68	0.30	0.33	0.02	0.03

Taking into account the conditions to be fulfilled by the amorphous coating materials, the practical choices were the alloys presented in Table 2.

The chemical composition of the coating layers with markings A1, A2 and A3 are shown in table 3.

Table 2. Coating alloys

Coating alloy	Marking
Fe80B20	A1
Fe60Ni20B20	A2
Fe45Cr14Mn7Mo2W1B17P12Si2	A3

Table 3. The chemical composition of the coating layers

Element		Chemical composition (atomic percentage)		
		Specimen marking		
		A1	A2	A3
B	Min.	3.94	7.92	2.23
	Max.	4.49	8.61	2.65
Cr	Min.	-	0.27	1.96
	Max.	-	0.34	2.42
Fe	Min.	15.68	23.56	6.85
	Max.	17.52	25.12	7.89
Ni	Min.	-	7.36	-
	Max.	-	8.61	-
Mn	Min.	-	0.06	0.95
	Max.	-	0.09	1.14
Mo	Min.	0.02	0.02	0.44
	Max.	0.03	0.03	0.59
P	Min.	0.01	0.01	0.02
	Max.	0.03	0.03	0.03
Si	Min.	0.03	0.02	0.28
	Max.	0.06	0.05	0.41
W	Min.	-	-	0.21
	Max.	-	-	0.34
Zn	Min.	0.04	0.09	0.03
	Max.	0.10	0.13	0.04
Zr	Min.	0.02	0.02	0.02
	Max.	0.03	0.03	0.03
Al	Min.	76.57	65.79	81.36
	Max.	80.39	58.60	84.11

3. Macro- microstructural evaluation of the layer - base material combination

The macroscopic examination of the coating layers show the main aspects regarding the coating techniques using plasma jet thermal spraying methodology. The macroscopic aspect of the coating layers is illustrated in Figures 1 ÷ 3.

Figure 1. A1.

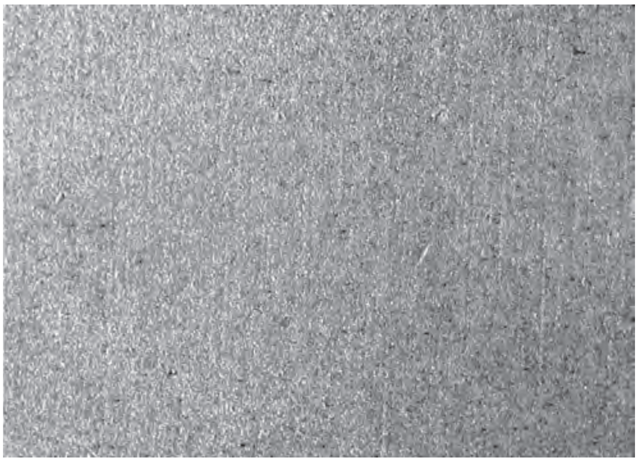

Figure 2. A2.

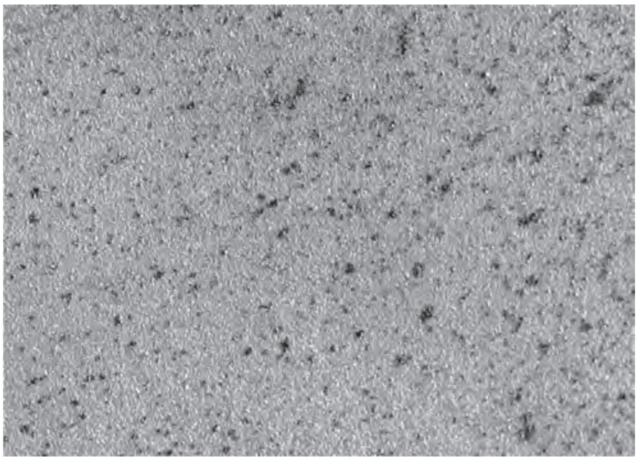

Figure 3. A3.

No cracks are observed on the deposited surface, but one can observe fine pores.

The microstructures of the deposited layers have been determined on transversal metalographic specimens, according to EN1321, using a MeF2 optical microscope.

The chemical attack used to put in evidence the microstructure does correspond to the norm CR12361. The microscopic examinations have been carried out according to SREN 1321 in the areas characteristic for the layers deposited by plasma jet thermal spraying.

The following microstructures are put in evidence:

- in the case of the base material (BM) one does observe a solid α solution with fine oxides particles (Figures 4, 6 and 8);
- in the case of the coating material (CM) A1 one does observe a granular structure with fine pores and Fe-B particles (Figure 5);

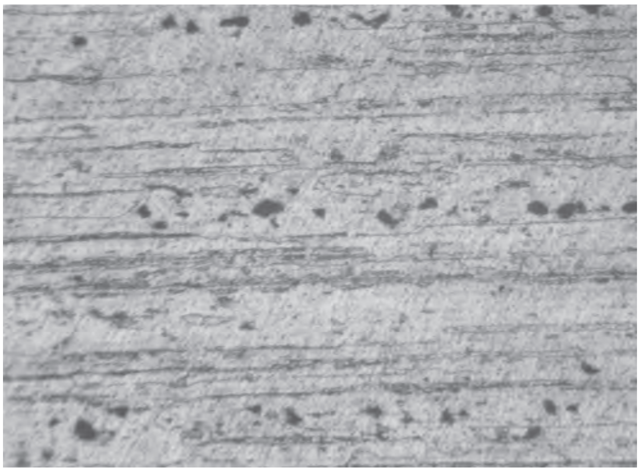

Figure 4. A1, BM, [Etching F7, 100×].

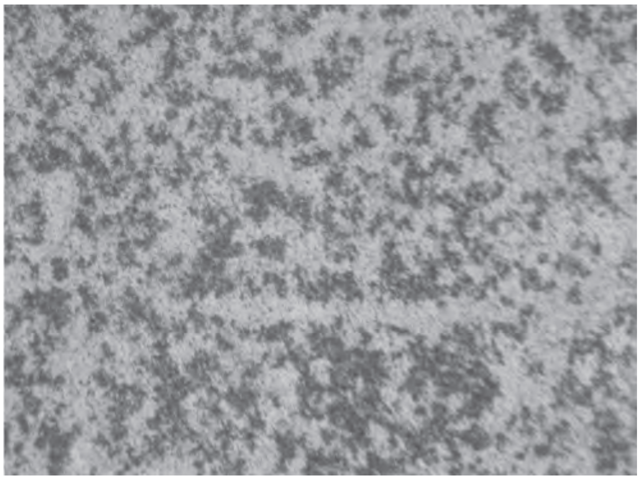

Figure 5. A1, CM, [Etching B8, 100×].

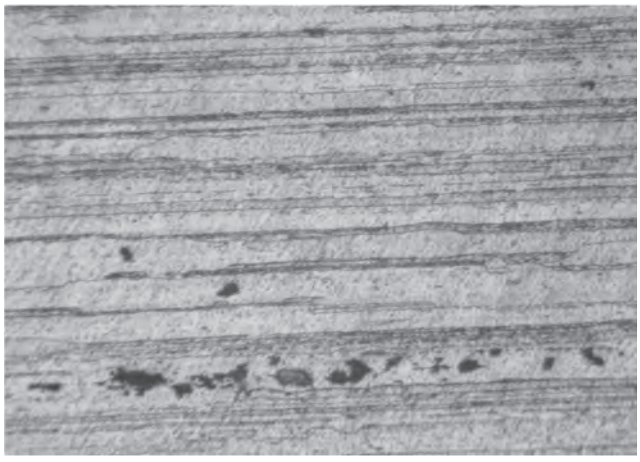

Figure 6. A2, BM, [Etching F7, 100×].

- in the case of the coating material A2 one does observe a granular structure with fine pores and complex Fe-Ni-B particles (Figure 7);
- in the case of the coating material A3 one does observe a granular structure with fine pores and complex Fe-B and Fe-P type particles, and intermetallic Fe-Cr and Fe-Mn particles (Figure 9).

Figure 7. A2, CM, [Etching B8, 100×].

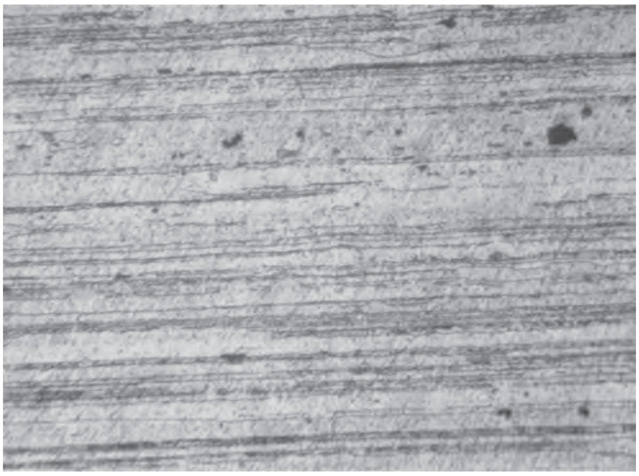

Figure 8. A3, BM, [Etching F7, 100×].

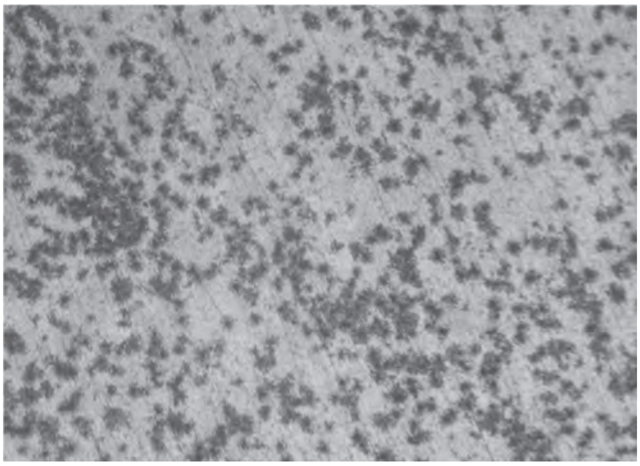

Figure 9: A3, CM, [Etching B8, 100×].

By analyzing the presented microstructures one does observe the presence of oxides and pores embedded into the structures, elements that cannot be put in evidence during the coating period due to the fact that the process is taking place in atmospheric conditions.

No cracks were observed on the analysed microstructures.

4. Quantitative evaluation of the coating layers using digital image processing

An 1875 x 1365 (pixels) area was selected from the image A1 of the coating layer (Figure 5) captured from the optical microscope. This image was pre-processed, segmented and binarized using 2 methods available in the implementation of the open-source imaging system ImageJ (as shown in Figures 10, 11and 12).

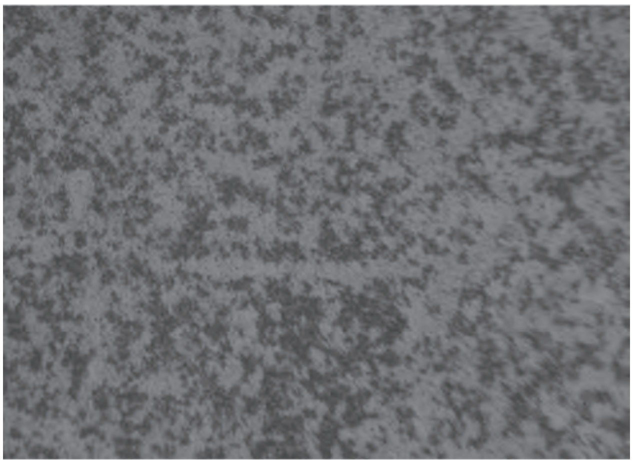

Figure 10. Selection cut from image 5.

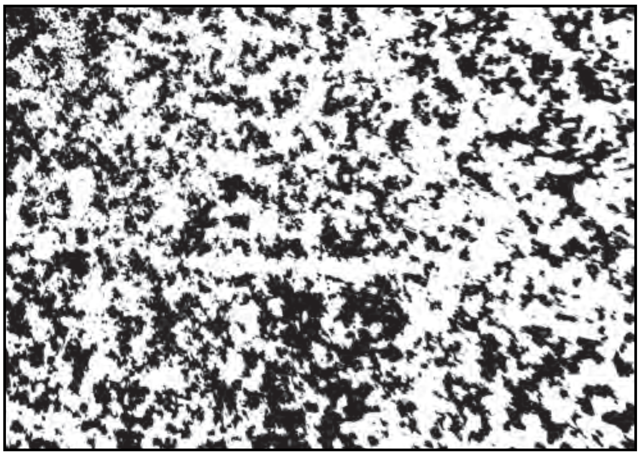

Figure 11. Image in Figure 10, binarized (method A).

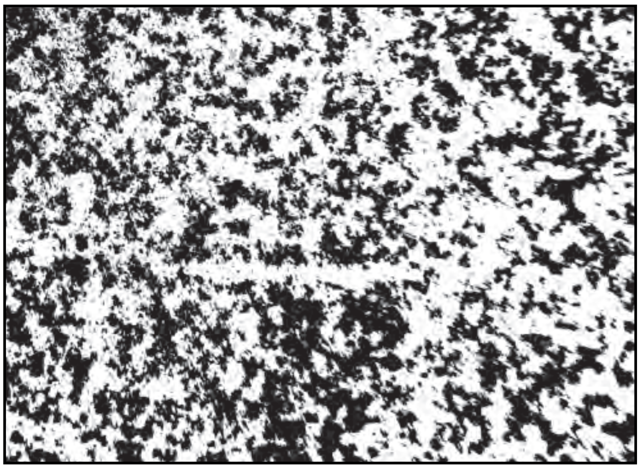

Figure 12. Image in Figure 10, binarized (method B).

To determine the percentage of the constituents the histograms of the binarized images were evaluated, the results being shown in table 4. Similar procedures were applied for the A2 images (Figure 7, from which an 1839 x 1263 area was selected - together with Figures 13, 14 and 15) and A3 (Figure 9, from which an 1893 x 1212 area was selected - together with Figures 16, 17 and 18).

Table 4. Results of the binarized images

Figure	White		Black	
	Microstructure	**Quantity [%]**	**Microstructure**	**Quantity [%]**
3.11	granular structure	58	Pores + Fe-B particles	42
3.12	granular structure	56.46	Pores + Fe-B particles	43.54
3.14	granular structure	68.4	Pores + Fe-Ni-B particles	31.6
3.15	granular structure	68	Pores + Fe-Ni-B particles	32
3.17	granular structure	65.12	Pores + Fe-B, Fe-P, Fe-Cr, Fe-Mn complex particles	34.88
3.18	granular structure	64.9	Pores + Fe-B, Fe-P, Fe-Cr, Fe-Mn complex particles	35.1

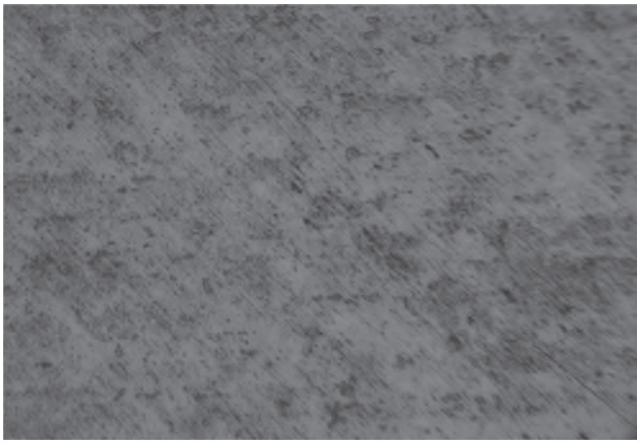

Figure 13. Selection cut from image 7.

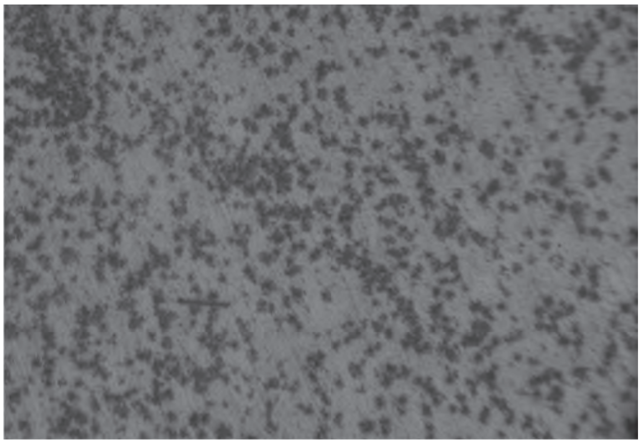

Figure 16. Selection cut from image 9.

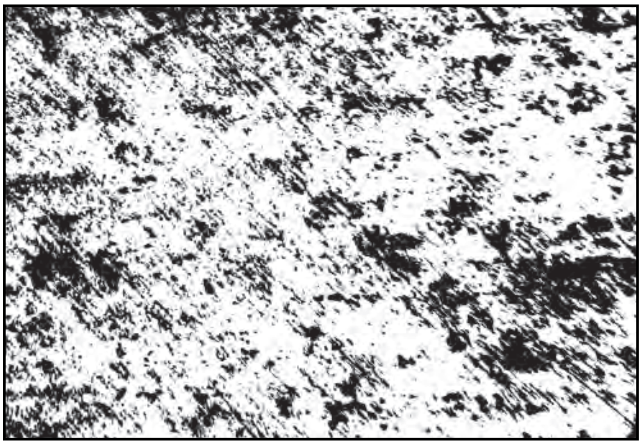

Figure 14. Image in Figure 13, binarized (method A).

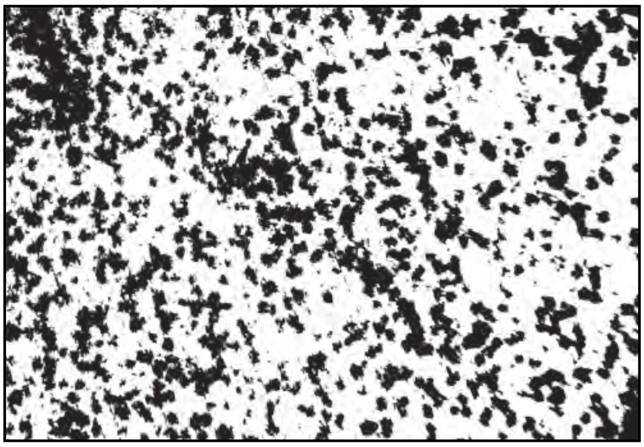

Figure 17. Image in Figure 16, binarized (method A).

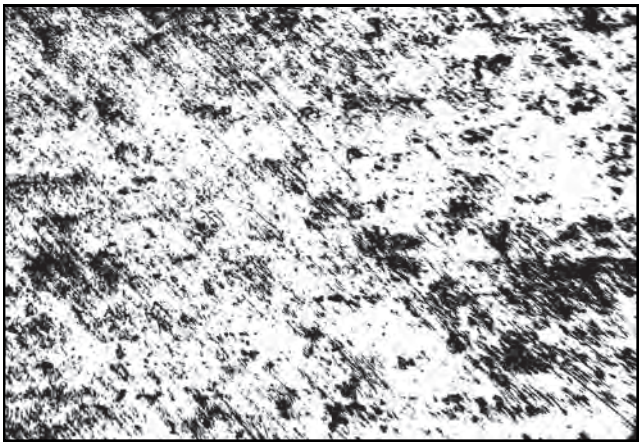

Figure 15. Image in Figure 13, binarized (method B).

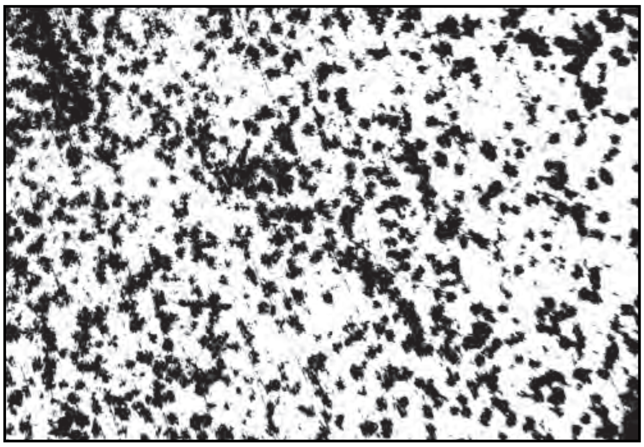

Figure 18. Image in Figure 16, binarized (method B).

5. Conclusions

Amorphous layers can be obtained by plasma jet thermal spraying. The materials used for experiments were aluminium as base material, due to its high thermal conductivity, and powders with a favourable composition were used as coating alloys.

The coating layers were investigated from a structural point of view, by chemical analysis and macro-microstructural analysis. The analyze of the coating layers microstructures revealed the presence of oxides in the structure, and no micro-cracking has been observed.

Given the specific steps and stages of microstructural analysis, in the experimental programmed carried out at ISIM Timisoara the specific imaging techniques like pre-processing, segmentation, binarization and histogram analysis were successfully used to obtain quantitative evaluation results.

Bibliography

[1]. Zang C., Guo R.Q., Yang Y., Wua Y., Liu L.: Influence of the size of spraying powders on the macrostructure and corrosion resistance of Fe-based amorphous coating, Electrochemica Acta, Vol. 56, 2011, pp. 6380-6388

[2]. Liua X.Q., Zhengb Y.G., Changa X.C., Houa W.L., Wanga J.Q., Tangc Z., Burgessc A.: Microstructure and properties of Fe-based amorphous metallic coatings produced by high velocity plasma spraying, Journal of Alloys and Compounds, Vol. 484, 2009, pp. 300-307

[3]. Zhou Z., Wang b L., Wang F.C., Hou H.F., Liu W., Wang J.Q.: Formation and corrosion behavior of Fe-based amorphous metallic coatings by HVOF thermal spraying, Surfaces & Coatings Technology, Vol. 204, 2099, pp. 563-570

[4]. Ni H.S., Liu X.H., Chang X.C., Hou W.L., Liu W., Wang J.Q.: High performance amorphous steel coating prepared by HVOF thermal spraying, Journal of Alloys and Compounds, 2009, pp. 163-167

[5]. Chokethawai K., McCartney D.G., Shipway P.H.: Microstructure evolution and thermal stability of an Fe-based amorphous alloy powder and thermally sprayed coatings, Journal of Alloys and Compounds, Vol. 480, 2009, pp. 351-359